REPORT D̄ ~~ ~~ AD-A247 983

Public reporting burden for this collection of informa... maintaining the data needed, and completing and rev... for reducing this burden, to Washington Headquarte... the Office of Management and Budget, Paperwork...

...wing instructions, searching existing data sources, gathering and ...y other aspect of this collection of information, including suggestions ...on Davis Highway, Suite 1204, Arlington, VA 22202-4302, and to

1. Agency Use Only (Leave blank).	2. Report Date. 1991	3. Report Type and Dat s Covered. Final - Journal Article

4. Title and Subtitle.
The Corrosion Behavior of Stainless Steels and Copper Alloys Exposed to Natural Seawater

6. Author(s).
B. J. Little and F. B. Mansfeld*

5. Funding Numbers.
Contract

Program Element No.	0601153N
Project No.	3102
Task No.	040
Accession No.	DN094463
Work Unit No.	13330A

7. Performing Organization Name(s) and Address(es).
Naval Oceanographic and Atmospheric Research Laboratory
Ocean Science Directorate
Stennis Space Center, MS 39529-5004

8. Performing Organization Report Number.
JA 333:027:91

9. Sponsoring/Monitoring Agency Name(s) and Address(es).
Naval Oceanographic and Atmospheric Research Laboratory
Basic Research Management Office
Stennis Space Center, MS 39529-5004

10. Sponsoring/Monitoring Agency Report Number.
JA 333:027:91

11. Supplementary Notes.
*University of Southern California, Los Angeles, CA 90089-0241
Published in Werkstoffe und Korrosion

DTIC
ELECTE
MAR 1992
S
C
D

12a. Distribution/Availability Statement.
Approved for public release; distribution is unlimited.

12b. Distribution Code.

13. Abstract (Maximum 200 words).

The corrosion behavior of stainless steels, titanium, and copper alloys exposed to flowing Pacific Ocean water was characterized using surface analytical and electrochemical techniques. Biofilm formation on stainless steels and titanium resulted in thin films of bacteria and diatoms that did not cause significant changes of the corrosion potential (E_{corr}) or surface properties. Rotating cylinder experiments indicated that both E_{corr} and corrosion rates for stainless steels and titanium were independent of mass transport. Four surface layers were identified on copper-containing materials: substratum metal; and inorganic chloride corrosion layer that contained alloying elements; a biofilm; and crystalline, spherical phosphate-rich deposits. All copper surfaces were colonized by bacteria independent of alloy composition. The complexity of the impedance spectra for copper-containing materials was attributed to formation of surface layers and contributions of charge transfer and mass transport controlled reactions mediated by the layers. Both anodic and cathodic reactions for copper-based materials were affected by mass transport.

14. Subject Terms.
Biofouling, corrosion, biodeterioration, electrochemistry

15. Number of Pages.
10

16. Price Code.

17. Security Classification of Report. Unclassified	18. Security Classification of This Page. Unclassified	19. Security Classification of Abstract. Unclassified	20. Limitation of Abstract. SAR

The corrosion behavior of stainless steels and copper alloys exposed to natural seawater

Korrosionsverhalten von nichtrostenden Stählen und Kupferlegierungen in natürlichem Meerwasser

B. J. Little* and F. B. Mansfeld**

Dedicated to Professor Dr. Ewald Heitz on the occasion of his 60th birthday

The corrosion behavior of stainless steels, titanium and copper alloys exposed to flowing Pacific Ocean water was characterized using surface analytical and electrochemical techniques. Biofilm formation on stainless steels and titanium resulted in thin films of bacteria and diatoms that did not cause significant changes of the corrosion potential (E_{corr}) or surface properties. Rotating cylinder experiments indicated that both E_{corr} and corrosion rates for stainless steels and titanium were independent of mass transport. Four surface layers were identified on copper-containing materials: substratum metal; an inorganic chloride corrosion layer that contained alloying elements; a biofilm; and crystalline, spherical phosphate-rich deposits. All copper surfaces were colonized by bacteria independent of alloy composition. The complexity of the impedance spectra for copper-containing materials was attributed to formation of surface layers and contributions of charge transfer and mass transport controlled reactions mediated by the layers. Both anodic and cathodic reactions for copper-based materials were affected by mass transport.

Das Korrosionsverhalten von nichtrostenden Stählen, Titan- und Kupferlegierungen in strömendem Meerwasser (Stiller Ozean) wurde mit Hilfe von Oberflächenanalysen und elektrochemischen Methoden untersucht. Die auf nichtrostendem Stahl und Titan entstehenden dünnen Biofilme bestanden aus Bakterien und Diatomäen, die das Korrosionspotential (E_{corr}) und die Oberflächeneigenschaften nicht signifikant veränderten. Versuche mit rotierendem Zylinder zeigten, daß sowohl das Korrosionspotential als auch die Korrosionsgeschwindigkeit von nichtrostendem Stahl und Titan unabhängig vom Stofftransport sind. Auf kupferhaltigen Werkstoffen wurden vier Oberflächenschichten nachgewiesen: metallisches Substrat; eine aus anorganischen Chloriden bestehende Korrosionsschicht mit Legierungselementen; ein Biofilm und kristalline kugelige, phosphatreiche Ablagerungen. Alle Kupferoberflächen wurden, unabhängig von der Legierungszusammensetzung, von Bakterien bevölkert. Der komplexe Charakter der Impedanzspektren der kupferhaltigen Werkstoffe wurde der Bildung von Oberflächenschichten und dem Beitrag von durch Ladungsübergang und Stofftransport kontrollierten Reaktionen durch die Oberflächenschichten zugeschrieben. Sowohl die anodische als auch die kathodische Reaktion der kupferhaltigen Werkstoffe wurde jedoch vom Stofftransport beeinflußt.

92-06617

92 3 13 022

Introduction

Realization that microorganisms can profoundly change the rates of the partial electrochemical reactions of a corrosion process and even its mechanism has led to renewed interest in the evaluation of corrosion behavior for structural materials in seawater. Investigators have reported an ennoblement of corrosion potential (E_{corr}) for stainless steels [1–3], titanium [2], platinum [2] and copper alloys [4] after exposure to natural seawater. Measurements of a mixed potential such as E_{corr} do not provide detailed mechanistic information, so little progress has been made in the interpretation of the reported ennoblements [5, 6].

The structure and composition of biofilms formed in natural seawater is often determined using scanning electron microscopy (SEM) coupled with energy dispersive X-ray analysis (EDS). However, Little et al. [7], using an environmental scanning electron microscope (ESEM) with EDS, have demonstrated that the number and types of microorganisms on surfaces have been underestimated by traditional SEM techniques. Preparation and dehydration cause fragile copper corrosion layers to slough from the surface, removing attached bacteria. Solvent extraction of water during SEM preparation also removes extracellular polymers and reduces the concentration of polymer-bound metals.

In this paper, electrochemical and ESEM/EDS data for three stainless steels, titanium, and five copper alloys are compared after exposure to natural seawater. We attempted to separate the effects of biofilms and corrosion products on corrosion kinetics by conducting experiments in both natural and abiotic artificial seawater. Measurements of E_{corr} vs. time, electrochemical impedance at E_{corr} and

*   Dr. *Brenda J. Little*, Naval Oceanographic and Atmospheric Research Laboratory, Stennis Space Center, MS 39529-5004, USA.
** Prof. *Florian B. Mansfeld*, Dept. of Materials Science, University of Southern California, Los Angeles, CA 90089-0241, USA.

determination of the corrosion kinetics as a function of mass transport [8] were used to monitor electrochemical behavior of the metals. Surface topography, biofilm formation and surface chemistry were documented.

Experimental

Three stainless steels – SS304, SS316 and SSAL6X, titanium-grade 2, and five copper-based materials – 99Cu (CDA 110), 90Cu:10Ni (CDA 706), 70Cu:30Ni (CDA 715), admiralty brass (CDA 443) and aluminum bronze (CDA 614) were exposed to flowing natural seawater at the Naval Civil Engineering Laboratory in Port Hueneme, California and to artificial seawater (Instant Ocean®, Aquarium Systems, Mentor, OH) at the Corrosion and Environmental Effects Laboratory (University of Southern California, Los Angeles, CA). Composition of the materials is given in Table 1. Samples were exposed in natural seawater at open-circuit potential (E_{corr}) as previously described [9, 10]. Metal coupons ($10.0 \times 0.6 \times 0.1$ cm each) were placed in a plastic holder such that there was minimal contact area between coupon and holder to reduce the possibility of crevice corrosion. Exposure periods ranged from 1 week to several months. Electrochemical impedance spectroscopy (EIS) data were collected in natural and artificial seawater at E_{corr} using a separate specimen for each measurement. Surface analysis was performed subsequently for the same sample. Impedance spectra were obtained with a Solartron model 1250 Frequency Response Analyzer and a Solartron model 1286 potentiostat.

Electrochemical dc measurements were made as a function of exposure time in natural and artificial seawater using a rotating cylinder electrode (RCE) [8] to evaluate the effects of mass transport [8]. RCE measurements made in the vicinity of E_{corr} were used to determine polarization resistance (R_p) as a function of rotation speed (r) after 2 h. Polarization curves for longer exposures were recorded for copper-based materials in the potential region E_{corr} ± 30 mV. Anodic and cathodic Tafel slopes (b_a and b_c, respectively) and corrosion current density (i_{corr}) were derived from these measurements using the software program POLFIT [11], an improved version of POLCURR [12]. A detailed study of the effect of mass transport on the anodic and cathodic reactions in the corrosion process is on-going for copper-based materials [13]. Polarization curves are determined in the vicinity of E_{corr} as a function of r for electrodes exposed to natural and artificial seawater for up to 12 weeks at a potential scan rate of 0.1 mV/sec.

Surface topography, biofilm distribution and surface chemistry were documented with ESEM/EDS. Exposed surfaces were fixed in 4% glutaraldehyde in filtered seawater, rinsed through saltwater/distilled water washes to distilled water and examined directly in the ESEM without further preparation or manipulation. ESEM examination was performed in an Electroscan (Wilmington, MA) Type II environmental scanning electron microscope. Specimens were attached to a Peltier stage maintained at 4 °C and imaged in an environment of water vapor at 2–5 torr to maintain samples in a hydrated state. The ESEM was operated at 20 keV using an environmental secondary detector. EDS data were obtained with a Tracor Northern (Middleton, WI) System II analyzer equipped with a diamond window light element detector. Samples were held at a 37.4° tilt during spectrum acquisition. A program correcting for atomic number (Z) [14], absorption (A) [15], and fluorescence (F) [16] was used for semiquantitative analysis during data acquisition. A complete review of ZAF correction procedures has been prepared by *Beaman* and *Isasi* [17].

Results

E_{corr} measurements for three stainless steels and titanium exposed to natural Pacific Ocean water and abiotic artificial seawater showed small shifts in the noble or positive direction [9, 10]. Four sets of SS304 exposed under natural and reduced light at different times of the year indicate that environmental conditions had no impact on E_{corr} (Fig. 1). Impedance spectra for three stainless steels and titanium for exposure periods between 5 and 124 days (d) were largely capacitive and did not show significant changes with alloy composition or exposure time (Fig. 2). Analysis of the
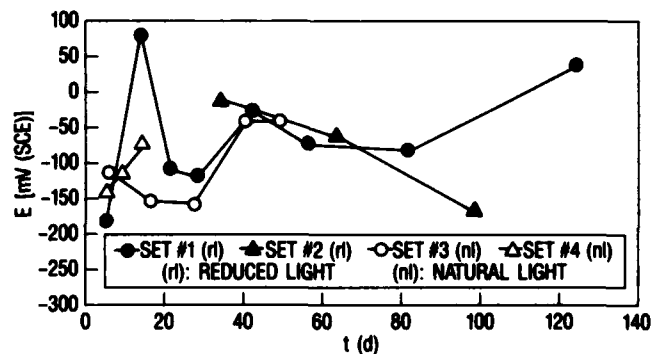

Fig. 1. Time dependence of E_{corr} for four sets of SS304 exposed to natural seawater

Abb. 1. Zeitlicher Verlauf des Korrosionspotentials E_{corr} für vier Sätze von SS304 in natürlichem Meerwasser

Table 1. Alloy compositions (weight %)
Tabelle 1. Legierungszusammensetzungen (Gew.-%)

|	UNS¹ No.	Cu	Ni	Zn	Al	Fe	Sn	Mn	Mo	Cr	C	Si	P	S	N	Ti
Copper	C11000	99.9 Oxygen Free														
90Cu:10Ni	C70600	86.73–87.02	10.47–10.81			1.68–1.69		0.58–0.67								
70Cu:30Ni	C71500	70.24	29.20			0.45		0.02								
Admiralty Brass	C44300	72.10		26.96		0.04	0.9									
Aluminum Bronze	C61400	90.37			6.87	2.37										
SS304	S30400		8.0 –10.5			REM		2.00		18.0–20.0	0.08	1.00	0.045	0.03	0.10	
SS316	S31600		10.0 –14.0			REM		2.00	2.0–3.0	16.0–18.0	0.08	1.00	0.045	0.03	0.10	
SSAL6X	N08366		23.5 –25.5			REM		2.00	6.0–7.0	20.0–22.0	0.03	1.00	0.03	0.03		
Ti Grade 2	R50400					0.30					0.10				0.03	REM
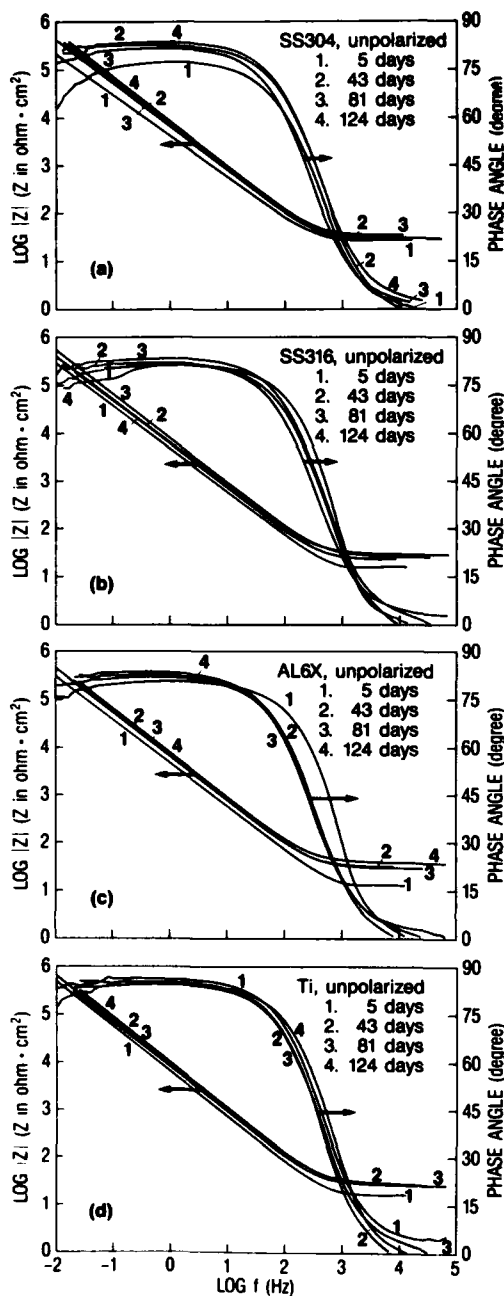
Fig. 2. Impedance spectra for SS304, SS316, AL6X and Ti grade 2 as a function of exposure time to natural seawater

Abb. 2. Impedanzspektren von SS304, SS316, AL6X und Titan Grade 2 in Abhängigkeit von der Auslagerungsdauer in natürlichem Meerwasser

Fig. 3. Time dependence of the electrode capacitance C_{dl} for four sets of SS304 exposed to natural seawater

Abb. 3. Zeitlicher Verlauf der Elektrodenkapazitanz C_{dl} für vier Sätze von SS304 in natürlichem Meerwasser

EIS data for four sets of SS304 in Fig. 2 indicate that electrode capacitance (C_{dl}) decreased slightly with exposure time (Fig. 3). The decrease was similar to that observed in abiotic seawater. R_p exceeded 10^6 ohm $\cdot$ cm^2 for stainless steel and titanium samples, indicative that there was no localized corrosion. Biofilms formed within 5 days and gradually increased in areal coverage, thickness and complexity. Bacteria dominated the biofilms with some attached diatoms (Fig. 4).

E_{corr} did not change significantly with exposure time for copper-containing materials exposed in natural seawater (Fig. 5). Impedance spectra were complicated and varied
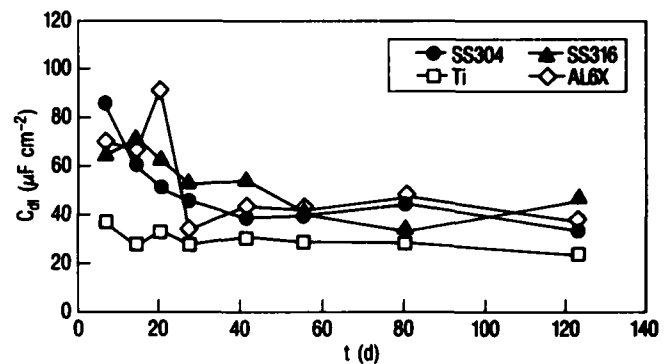
with alloy composition, exposure time and biofilm formation. The most notable feature in the spectra for 99Cu exposed in natural seawater was increased impedance in the high frequency region with exposure time (Fig. 6a) and the appearance of two persistent time constants after about 7 weeks (Fig. 6b). The surface of 99Cu was covered with a loosely adherent corrosion layer that contained 2–8% chloride. The wet layer detached from the substratum metal in several locations (Fig. 7). The corrosion product layer was covered with a gelatinous biofilm containing numerous bacteria and crystalline spherical deposits after 3 weeks (Fig. 8a & b). The crystalline deposits were predominantly copper, calcium and phosphorus (Fig. 9a & b). Impedance spectra for 99Cu were different in natural (Fig. 6) and artificial seawater (Fig. 10). The pronounced increase of the impedance with exposure time observed in natural seawater (Fig. 6) did not occur in artificial seawater. The most obvious difference in the surface deposits formed in the two media was the biofilm containing bacteria and their polymeric exudates on surfaces exposed to natural seawater. Surfaces exposed in abiotic artificial seawater were covered by a chloride corrosion layer. The weight percent of the surface bound chlorine after exposure to abiotic media ranged from 4–10. Phosphate-rich crystalline spheres formed in both natural and artificial seawater at approximately the same exposure times and in the same concentration.

Impedance spectra for 70Cu:30Ni exposed in natural seawater did not show increased impedance at higher frequencies (Fig. 11a). The frequency dependence of the phase angle (Fig. 11b) suggests that two or three time constants determine the impedance. An influence of mass transport is indicated in the low frequency region. The surface of 70Cu:30Ni was covered with a tenacious layer of corrosion product. Bacteria were embedded within the corrosion layer after 3 weeks (Fig. 12). Spherical phosphorus-rich deposits could be located on the 70Cu:30Ni surface after 9 weeks. A steady increase of the impedance in the capacitive region was observed for 70Cu:30Ni exposed to artificial seawater (Fig. 13).

Impedance spectra for the other copper-containing materials in natural seawater were intermediate between those for 99Cu and 70Cu:30Ni and will not be presented. After 3 weeks all copper surfaces except 70Cu:30Ni were uniformly covered with a biofilm. The complexity and thickness of the biofilm increased with exposure time.
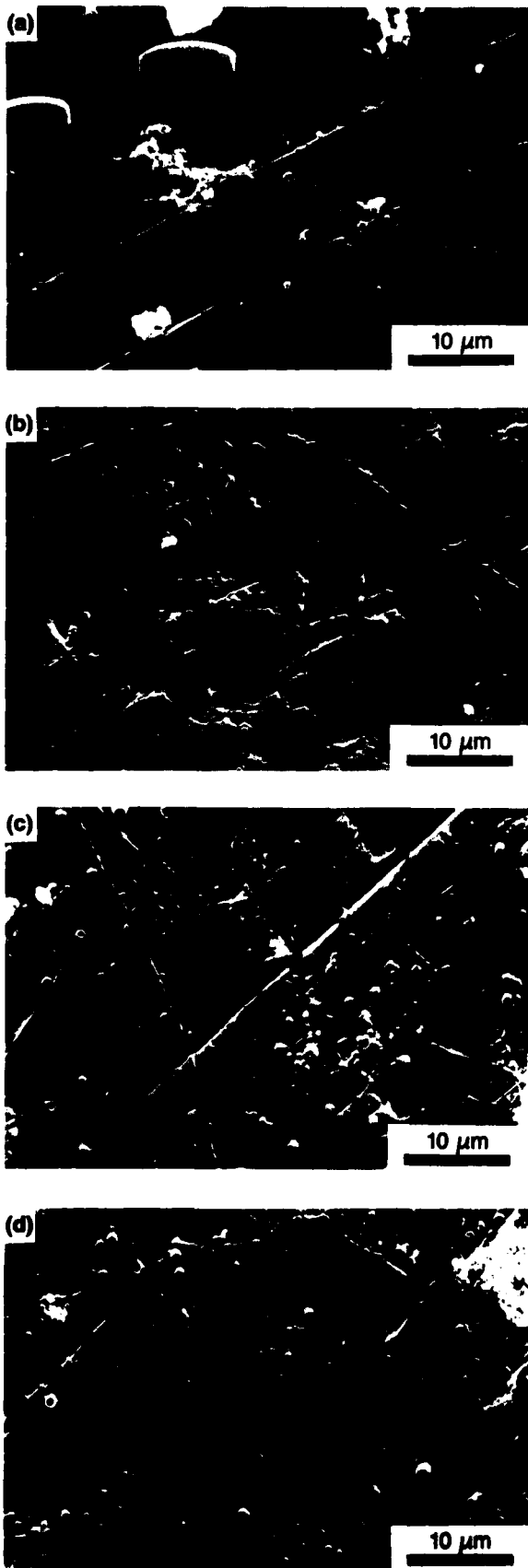
Fig. 4. Biofilms on a) 304SS, b) 316SS, c) AL6X, and d) Ti after 49 days in natural seawater

Abb. 4. Biofilme auf a) SS304, b) SS316, c) AL6X und d) Ti nach 49 Tagen in natürlichem Meerwasser
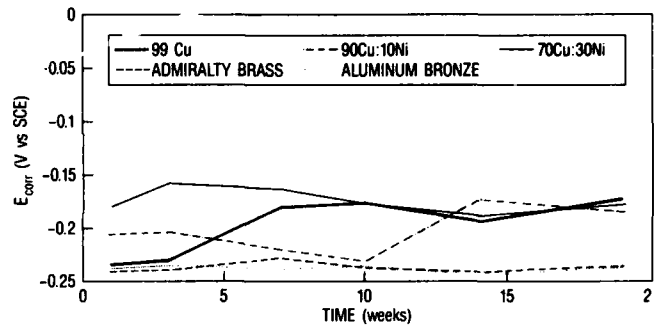

Fig. 5. E_{corr} vs. time for copper-containing materials exposed to natural seawater

Abb. 5. Zeitlicher Verlauf des Korrosionspotentials E_{corr} für kupferhaltige Werkstoffe in natürlichem Meerwasser
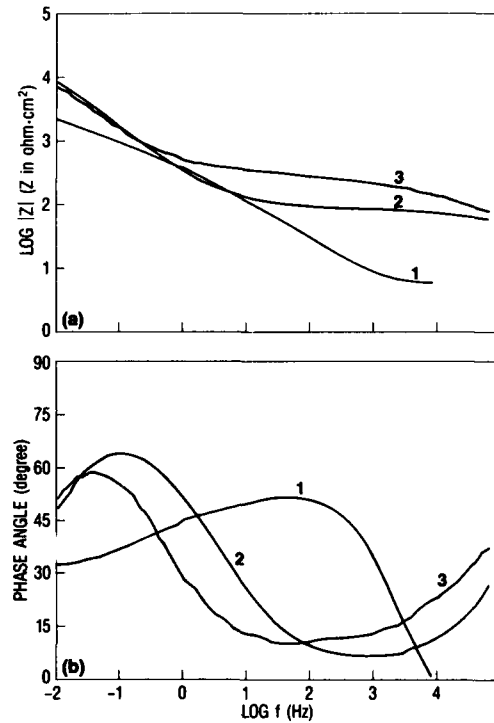

Fig. 6. Bode-plots for 99Cu as a function of exposure time to natural seawater. Exposure times: 1 week (curve 1), 7 weeks (curve 2) and 10 weeks (curve 3)

Abb. 6. Bode-Diagramme für 99Cu in Abhängigkeit der Auslagerungsdauer in natürlichem Meerwasser; Auslagerungsdauern: 1 Woche (Kurve 1), 7 Wochen (Kurve 2) und 10 Wochen (Kurve 3)

There was no indication of localized corrosion on any of the samples, either in the impedance data or in the surface imagery.

E_{corr} and R_p for the copper-containing metals were determined as a function of r in natural and artificial seawater using RCE. R_p was determined as the tangent of a polarization curve (potential (E) vs. current density (i)) at E_{corr} according to the following definition:

$$R_p = (dE/di)_{i = 0} \tag{1}$$

E_{corr} did not change significantly with increasing rotation speed (Fig. 14). Corrosion rate expressed as $1/R_p$ showed a
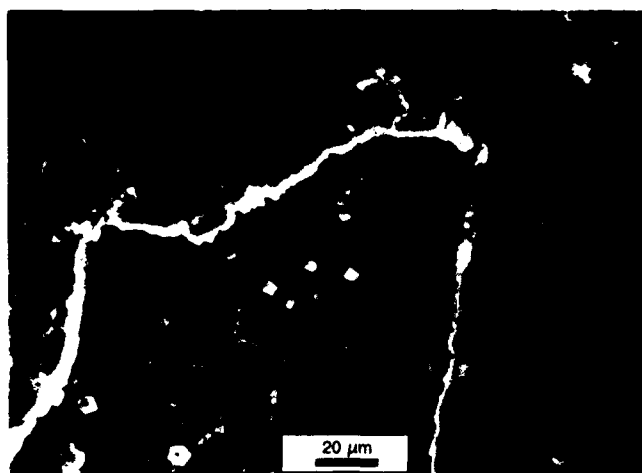
Fig. 7. Surface deposits on 99Cu and exposed substratum metal
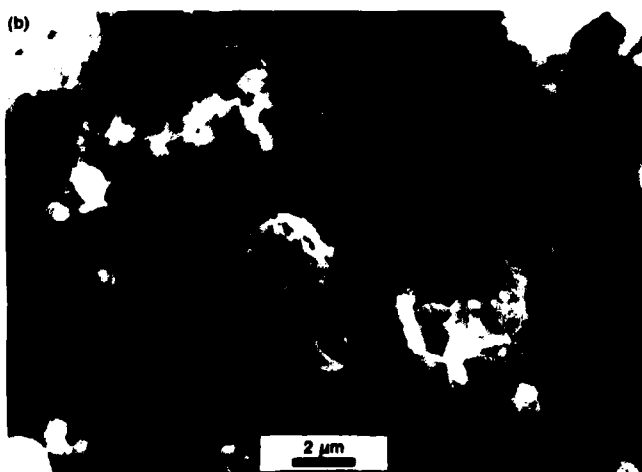**Abb. 7.** Ablagerungen auf der Oberfläche von 99Cu und freiliegendem Substrat

Fig. 9. a) Crystalline deposits on 99Cu. b) EDS spectrum for crystalline deposits
Abb. 9. a) Kristalline Ablagerungen auf 99Cu. b) EDS-Spektrum der kristallinen Ablagerungen

linear increase with $r^{0.7}$ [8]. Table 2 summarizes the results of the statistical analysis of the dependence of E_{corr} and $1/R_p$ on rotation speed (in rpm) expressed as follows:

$$E_{corr} = a_1 + a_2 \, r^{0.7} \tag{2}$$

and

$$1/R_p = b_1 + b_2 \, r^{0.7} , \tag{3}$$

where a_1 (in mV vs. SCE) is the value of E_{corr} for stagnant conditions ($r = 0$); b_1, the corresponding value for $1/R_p$ (in
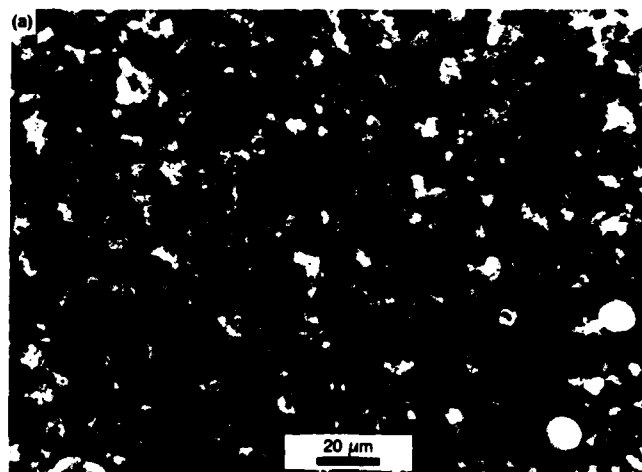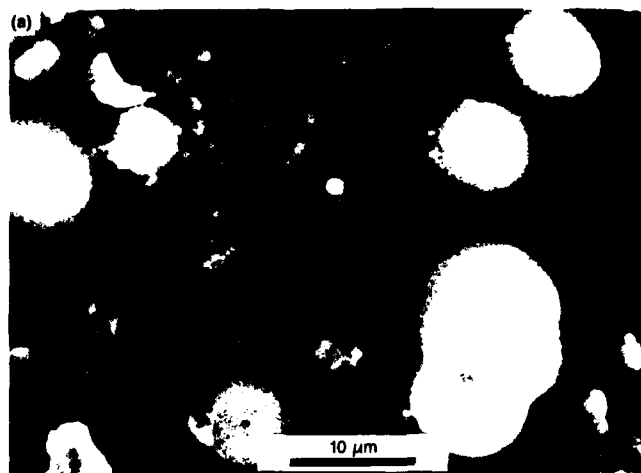

Fig. 8. a) Surface deposits on 99Cu after 7 weeks showing bacteria and crystalline deposits. b) Bacteria within biofilm on 99Cu after 7 weeks exposure to natural seawater

Abb. 8. a) Ablagerungen auf der Oberfläche von 99Cu nach 7 Wochen: Bakterien und kristalline Ablagerungen; b) Bakterien im Biofilm auf 99Cu nach 7 Wochen in natürlichem Meerwasser
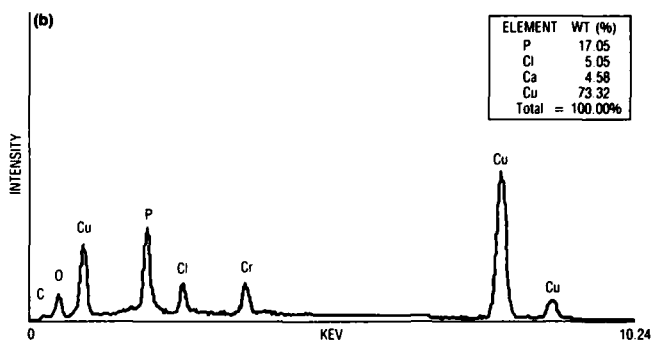
Table 2. Dependence of E_{corr} and $1/R_p$ on rotation speed of RCE
Tabelle 2. Abhängigkeit von E_{corr} und $1/R_p$ von der Drehzahl der rotierenden Zylinderelektrode

Material	E_{corr} (mV vs SCE)		$1/R_p$ (ohm^{-1} × cm^{-2})	
	a_1	a_2	b_1	b_2
99Cu	−226	−0.05	5.8×10^{-4}	7.8×10^{-6}
90Cu:10Ni	−229	−0.02	7.2×10^{-4}	3.3×10^{-6}
70Cu:30Ni	−201	−0.11	1.5×10^{-3}	1.1×10^{-5}
Aluminum Bronze	−241	−0.04	4.1×10^{-4}	7.9×10^{-6}
Admiralty Brass	−247	−0.10	6.7×10^{-4}	1.0×10^{-5}
SS304	−108	−0.06	1.1×10^{-5}	-4.5×10^{-9}
Ti Grade 2	−178	−0.01	1.3×10^{-6}	-6.8×10^{-10}

Fig. 12. Bacteria embedded in corrosion layer on 70Cu:30Ni after 3 weeks exposure to natural seawater

Abb. 12. In die Korrosionsschicht auf CuNi 70 30 nach dreiwöchiger Auslagerung in natürlichem Meerwasser eingebettete Bakterien
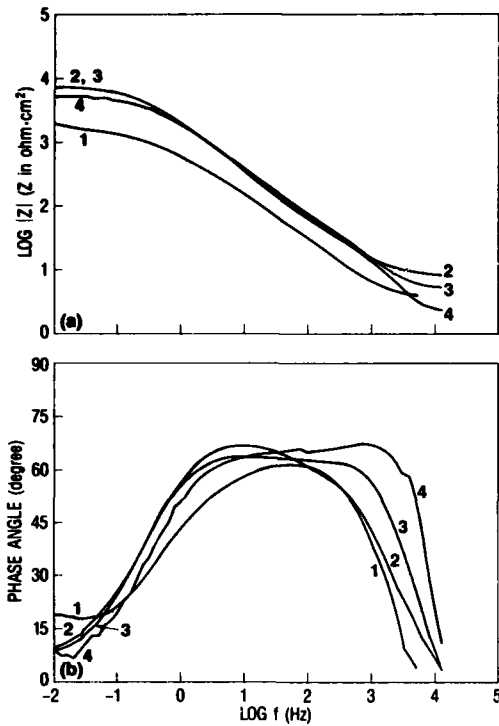
Fig. 10. Bode plots for 99Cu as a function of exposure time to artificial seawater. Exposure times: 1 day (curve 1), 3 weeks (curve 2), 5 weeks (curve 3) and 8 weeks (curve 4)

Abb. 10. Bode-Diagramme für 99Cu in Abhängigkeit von der Auslagerungsdauer in künstlichem Meerwasser; Auslagerungsdauern: 1 Tag (Kurve 1), 3 Wochen (Kurve 2), 5 Wochen (Kurve 3) und 8 Wochen (Kurve 4)
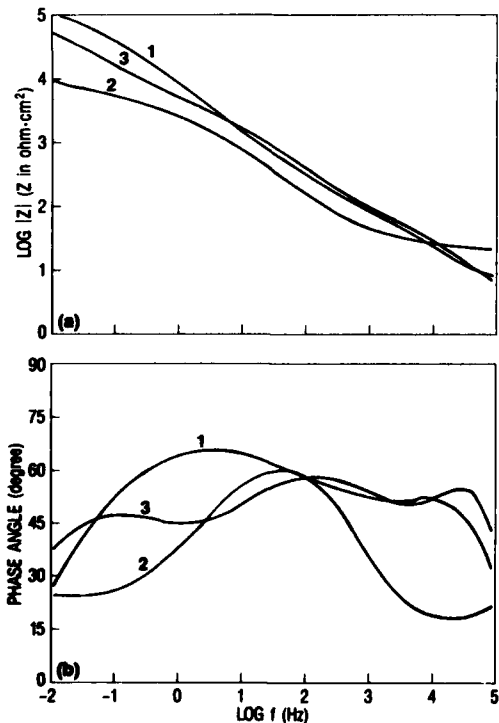

Fig. 13. Bode plots for 70Cu:30Ni as a function of exposure time to artificial seawater. Exposure times: 1 week (curve 1), 5 weeks (curve 2) and 8 weeks (curve 3)

Abb. 13. Bode-Diagramme für CuNi 70 30 in Abhängigkeit von der Auslagerungsdauer in künstlichem Meerwasser; Auslagerungsdauern: 1 Woche (Kurve 1), 5 Wochen (Kurve 2) and 8 Wochen (Kurve 3)

Fig. 11. Bode plots for 70Cu:30Ni as a function of exposure time to natural seawater. Exposure times as in Fig. 5

Abb. 11. Bode-Diagramme für CuNi 70 30 in Abhängigkeit von der Auslagerungsdauer in natürlichem Meerwasser; Auslagerungsdauern wie in Abb. 5
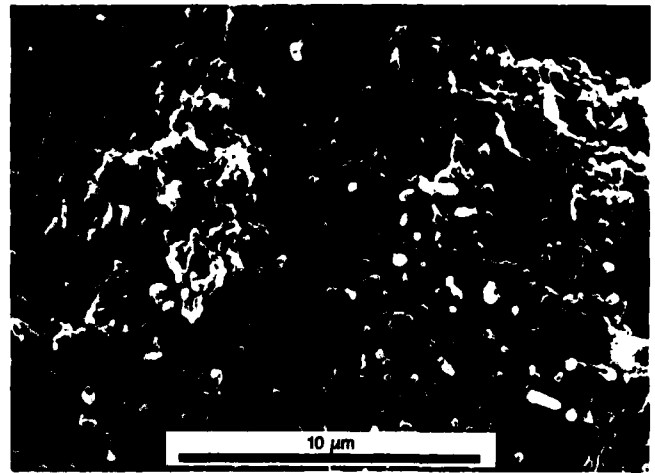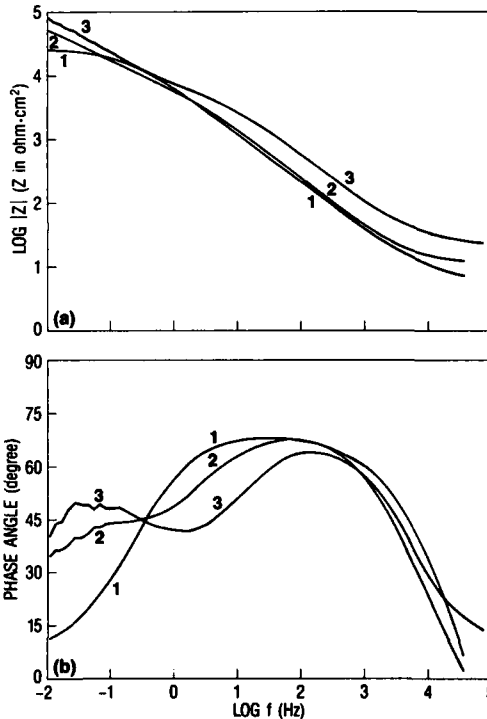
$ohm^{-1} cm^{-2}$); and a_2 and b_2 are the corresponding regression slopes. $1/R_p$ values for stainless steels and titanium did not depend on rotation speed (i.e. $b_2 \to 0$). E_{corr} was not significantly affected by mass transport for any of the materials. In all cases, (a_2) was close to zero.

In a series of experiments, potentiodynamic polarization curves were obtained in the vicinity of E_{corr} for copper-
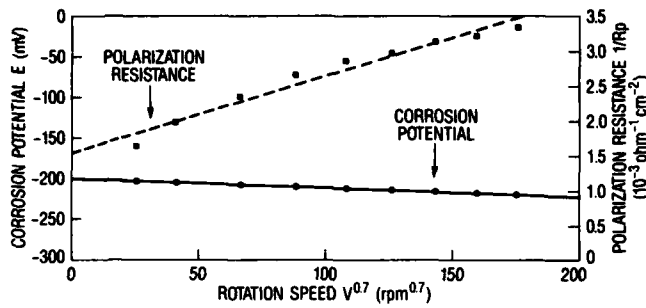
Fig. 14. Dependence of E_{corr} and $1/R_p$ on $r^{0.7}$ for 70Cu:30Ni exposed to artificial seawater for 2 h

Abb. 14. Abhängigkeit von E_{corr} und $1/R_p$ von $r^{0.7}$ für CuNi 70 30 nach 2 h in künstlichem Meerwasser

containing alloys exposed to natural and artificial seawater. Experimental data were fitted to Equation 4 which describes the relationship between E and i:

$$i = i_{corr} \{exp [2.3 (E - E_{corr})/b_a] - exp [2.3 (E_{corr} - E)/b_c]\} \qquad (4)$$

A comparison of an experimental polarization curve recorded at a r = 1600 rpm and a fitted curve for 99Cu after 7d in natural seawater shows excellent agreement between the two curves (Fig. 15). Fitted values of E_{corr} (Fig. 16a), b_a (Fig. 16b), b_c (Fig. 16c) and i_{corr} (Fig. 16d) are plotted vs. $r^{0.7}$ for 99Cu and 70Cu:30Ni after exposure to natural seawater for 7 and 21d. E_{corr} is independent of rotation speed except for 99Cu after 7d for which a slight decrease with r was observed. The anodic Tafel slope, b_a, falls between 40 and 80 mV suggesting that the anodic reaction is under mixed kinetic and diffusion control [18, 19]. A slight increase of b_a with r is indicated. The cathodic Tafel slope, b_c, is independent of r except for 99Cu after 21d, where a linear increase of b_c with $r^{0.7}$ is indicated. The i_{corr} is low and independent of r for 70Cu:30Ni at both 7 and 21d. In contrast, i_{corr} for 99Cu has much higher values and increases with time. A linear relationship between i_{corr} and $r^{0.7}$ is indicated.

Discussion

The electrochemical behavior of copper-containing alloys exposed to natural seawater was markedly different
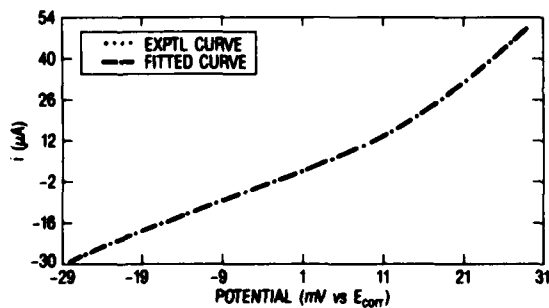

Fig. 15. Comparison of experimental and fitted polarization curves for 99Cu after exposure to natural seawater for 7 days; RCE. 1600 rpm

Abb. 15. Vergleich der experimentellen und der eingepaßten Polarisationskurven von 99Cu nach 7 Tagen in natürlichem Meerwasser; rotierende Zylinderelektrode. 1600 min⁻¹
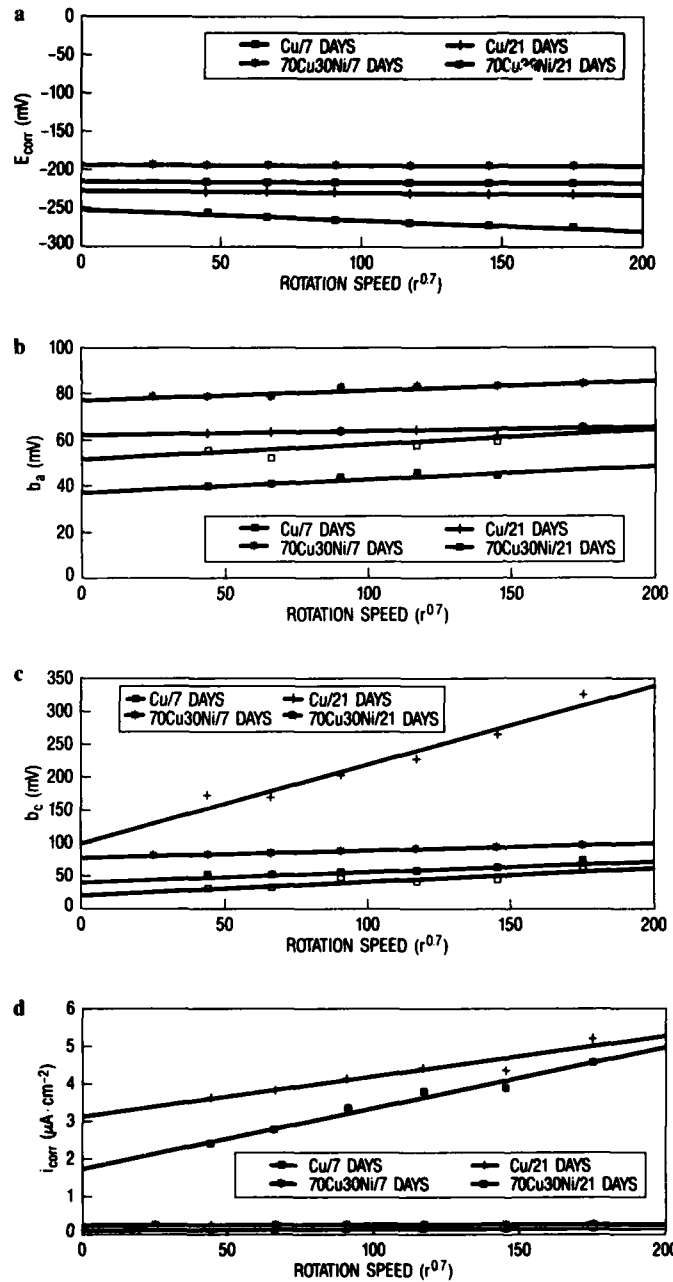

Fig. 16. Dependence of E_{corr} (Fig. 16a). b_a (Fig. 16b). b_c (Fig. 16c) and i_{corr} (Fig. 16d) on rotation speed of RCE for 99Cu and 70Cu:30Ni after exposure to natural seawater for 7d and 21d

Abb. 16. Abhängigkeit von E_{corr} (Abb. 16a). b_a (Abb. 16b). b_c (Abb. 16c) und i_{corr} (Abb. 16d) von der Drehzahl der rotierenden Zylinderelektrode aus 99Cu und CuNi 70 30 nach 7 und 21 Tagen in natürlichem Meerwasser

from that of stainless steels and titanium exposed under identical conditions. The corrosion potential E_{corr} and the impedance spectra for stainless steels and titanium did not change significantly as a function of alloy composition. exposure time or biofilm formation over 4 months. In contrast. impedance spectra for the copper-containing alloys varied with alloy composition. changed as a function of exposure time. and were altered by the presence of the biofilm.

Much attention has been paid to the ennoblement of E_{corr} for stainless steels during exposure to natural seawater [1–3]. The practical importance of ennoblement is the increased probability of localized corrosion as E_{corr} approaches the pitting potential (E_{pit}). Despite numerous investigations monitoring E_{corr}, a reasonable explanation for ennoblement has not been offered. The suggestion [20, 21] that ennoblement is the result of an acceleration of the rate of the oxygen reduction reaction under the biofilm has been confirmed experimentally [22]; however, the mechanism remains unresolved. Thermodynamic factors have been suggested as possible mechanisms, including increase of the partial pressure of oxygen under the biofilm and a decrease in interfacial pH. An increase in the partial pressure would move the reversible potential of the oxygen electrode in the noble direction, but cannot explain large shifts of E_{corr}. A local decrease in pH would produce the same effect. However, local acidification would move E_{pit} in the negative direction to potentials significantly below the reported E_{corr} values [6]. The cause for the sometimes observed ennoblement must therefore be of kinetic nature. *Johnsen* and *Bardal* [3] reported that E_{corr} approached – 50 mV after 28 d for stainless steels with molybdenum contents of 1–3 w/o. In contrast, E_{corr} for alloys containing 6 w/o molybdenum reached values between 50 and 150 mV vs. SCE. *Scott* et al. [23] reported that in laboratory studies stainless steels containing 6 w/o molybdenum were susceptible to microbiologically influenced corrosion while SS316L, containing 2%–3% molybdenum, was more resistant. These authors stated that "greatest corrosion occurred in the 6% Mo alloys ... and, surprisingly, type 316L performed the best with almost no detectable corrosion" [23]. Molybdenum may play a role in acceleration of the cathodic reaction leading to ennoblement of E_{corr} and local attack of stainless steels containing 6 w/o molybdenum. Organometallic catalysis of the oxygen reduction reaction has been proposed as the mechanism for increased oxygen reduction [24, 25], but has never been demonstrated.

In the present study an ennoblement of E_{corr} was not observed for stainless steels, titanium or copper-based materials. *Little* et al. [26] demonstrated that E_{corr} for 304 stainless steel exposed to natural seawater varied with interfacial pH and dissolved oxygen. Biofilm formation in Pacific Ocean water at Port Hueneme, California, did not impact interfacial chemistry to the extent that would cause a shift in E_{corr}. EIS and ESEM/EDS [7, 8] provide clear indications that localized corrosion did not occur on any of the samples exposed for time periods exceeding 4 months.

RCE experiments for stainless steels and titanium demonstrated that mass transport had no observed effect ($b_1 = 0$) on corrosion rates of these materials. Both corrode at very low rates in seawater because of the presence of a tenacious passive oxide layer. The cathodic reaction is under charge transport control and the passive current density is independent of transport of solution constituents. Therefore, both E_{corr} and corrosion rate are independent of mass transport.

Impedance spectra for stainless steels and titanium were not altered by biofilm formation during exposure to natural seawater. C_{dl} remained close to 30 μF/cm², the theoretical value for double layer capacitance. C_{dl} remained constant while the electrodes were progressively covered with a biofilm because the water-like structure of the biofilm is similar to the electrical double layer. Lack of change in impedance demonstrated that under the exposure conditions there was no localized corrosion over the four-month period.

A simple mechanism can be derived from EIS and RCE data for the electrochemical behavior of stainless steels and titanium in natural seawater in which both cathodic and anodic reactions are under charge transfer control. Corrosion rate equals the rate of passive film dissolution independent of potential and mass transport in the solution. Corrosion rates do not change even if E_{corr} increases due to biofilm formation unless the local chemistry under the biofilm becomes aggressive enough to increase the passive current density i_{pass}. When E_{corr} reaches E_{pit}, pitting or crevice corrosion will occur. Design considerations and local geometry play a major role in the initiation of crevice corrosion.

In contrast to the simple corrosion behavior of stainless steels and titanium in natural seawater, a more complicated behavior was exhibited by copper-based materials as evidenced in EIS and RCE data. Several authors reported the influence of corrosion products and mass transport on corrosion resistance of copper and its alloys in seawater [18, 19, 27, 28]. The additional effects of biofilm formation on the corrosion kinetics of these materials have been neglected.

E_{corr} did not change significantly for the copper alloys with exposure time, corrosion product formation or biofilm development. Corrosion rates for copper-based materials in abiotic artificial seawater after exposure for 2 h increased with r in the RCE experiments, but E_{corr} remained constant (Table 2). These results can be explained using mixed potential theory, showing that both the anodic and the cathodic partial reactions are mass transport controlled. Increased transport of Cl^- to the surface accelerates the anodic reaction:

$$Cu + 2Cl^- \rightarrow CuCl_2^- + e^- . \tag{5}$$

while increased transport of oxygen accelerates the cathodic reaction. As a result, E_{corr} remains independent of rotation speed, while corrosion rate increases. In the experiments listed in Table 2, freshly polished 70Cu:30Ni showed the highest corrosion rate as expressed qualitatively by $1/R_p$. Corrosion rates decreased rapidly for 70Cu:30Ni (Fig. 16d) and 90Cu:10Ni after 1 week reaching low values independent of mass transport. *Wood* et al. [19] observed that freshly polished 70Cu:30Ni had higher corrosion rates than freshly polished 99Cu. Corrosion rates for 99Cu, admiralty brass and aluminum bronze did not decrease to the same extent with time. E_{corr} and $1/R_p$ showed dependence on r similar to that reported in Table 2.

Anodic Tafel slopes shown in Fig. 16b for 99Cu and 70Cu:30Ni fall between 40 and 80 mV. *Kato* et al. [18] citing earlier literature suggested that a Tafel slope b_a of 60 mV can be attributed to a one-electron transfer reaction with diffusion of a reactant or product in the aqueous phase being the rate-determining step. It can be concluded that transport of Cl^- to or transport of $CuCl_2^-$ from the surface is the rate-determining step. *Mansfeld* and *Kenkel* [29] showed that anodic polarization curves for 99Cu shift to higher current density as r increased. *Wood* et al. [19] studied the corrosion kinetics of Cu and 70Cu:30Ni in flowing seawater for fresh and "filmed surfaces". The authors defined filmed surfaces as those on which corrosion layers had formed. By applying certain diagnostic criteria

for the flow dependence of the anodic current they determined that b_a was close to 60 mV in the vicinity of E_{corr} but changed to 120 mV at more anodic potentials. After prolonged exposure times the same analysis resulted in $b_a = 120$ mV in the vicinity of E_{corr} and $b_a = 60$ mV at more anodic potentials. The anodic Tafel slope for 70Cu:30Ni was about 120 mV in the vicinity of E_{corr}, but changed to 60 mV for a filmed surface after longer exposures. These results illustrate the complexity of the anodic dissolution mechanism for copper-based materials and the strong effects of corrosion product formation and mass transport on individual steps. Wood et al. [19] did not discuss possible effects of biofilm formation on corrosion kinetics despite the authors' stated concern to create realistic experimental conditions through the use of natural seawater with a steady-state bacterial population.

The complexity of the corrosion kinetics of copper-based materials demonstrated in dc data is reflected in the complicated shape of the impedance data. It has not been possible to perform quantitative analysis of EIS data using present models. Appropriate models must include mechanistic information from dc studies and surface analyses. Corrosion products of copper alloys are known to have different properties than those of pure copper [30] and can be expected to produce alloy-specific EIS spectra. Contributions of charge transfer, mass transport and biofilms must be included in models. The contribution of the phosphorous-rich spheres (Fig. 9) to the impedance spectra cannot be evaluated at this time. Gerchakov et al. [31] reported similar spherical crystalline phosphorus-rich structures on copper alloys exposed to natural seawater and speculated that the deposits might have nucleated at cathodic microcorrosion sites.

In a qualitative analysis of EIS data, it can be concluded that the frequency dependence of the impedance for 99Cu after 7 and 10 weeks exposure to natural seawater appears to be due to the presence and properties of the biofilm. Similar spectra have been reported for metals coated with porous polymers [32]. The decrease of the capacitance with exposure time for 70Cu:30Ni in natural seawater appears to be due to thickening of the surface layers, including the biofilm.

Copper alloys prevent or retard the settlement of macrofouling species including barnacles, mussels and tubeworms. However, bacteria, fungi and microalgae and their cellular exudates form a slime layer on copper-containing surfaces [33]. Marszalek et al. [34] using scanning electron microscopy (SEM) documented that copper-containing materials fouled at a slower rate than stainless steel surfaces and that the microflora on copper surfaces was less diverse than that found on steel and glass surfaces exposed under identical conditions.

Several authors have reported microbiologically influenced corrosion (MIC) of copper alloys in marine environments [35, 36]. Specific mechanisms for MIC of copper alloys include ammonium production [37], sulfide production [37, 38], under-deposit corrosion [34], acid production [37] and differential cells produced by metals bound by bacterial extracellular polymers [39]. While it is generally recognized that microorganisms can accelerate corrosion processes, the contributions of marine biofilms to specific electrochemical parameters other than E_{corr} have not yet been assessed. In this paper we have demonstrated that the formation of corrosion product layers and biofilms adds to the complexity of corrosion behavior as evidenced by complex impedance spectra for copper-containing materials.

Summary and Conclusions

No significant changes of E_{corr} or impedance spectra were observed for SS304, SS316, SSAL6X and titanium during immersion in Pacific Ocean water. The capacitive nature of impedance spectra proves that localized corrosion did not occur for exposure times up to 4 months. The electrode capacitance did not change as biofilms formed.

RCE experiments demonstrated that the anodic reaction for copper-based materials is under mixed control and the cathodic corrosion reaction is under mass transport control. As a result E_{corr} remained independent of rotation speed, while the i_{corr} increased for freshly polished surfaces after 2 h immersion in artificial seawater. Both E_{corr} and corrosion rates for stainless steels and titanium were independent of mass transport. Analysis of dc polarization curves for copper-based materials permits an evaluation of changes in corrosion kinetics (b_a, b_c, i_{corr} and E_{corr}) with exposure time in natural seawater.

Impedance spectra for copper-based materials exposed in natural seawater include contributions of corrosion layers, mass transport and biofilm formation in natural seawater. Because of the complicated nature of the spectra a quantitative analysis has not been possible. Comprehensive models for such an analysis are being developed. Qualitative analysis of EIS data shows that formation of the biofilm can be recognized in the impedance spectra for 99Cu after 7 weeks exposure. Similar changes of the impedance spectra for 70Cu:30Ni were not observed in the same time period. The surface of 99Cu was covered with a gelatinous biofilm containing bacteria and spherical crystalline deposits after 3 weeks in natural seawater. The surface of 70Cu:30Ni was covered with a tenacious corrosion product in which bacteria were embedded.

Acknowledgements

References

[1] S. C. Dexter, S. Lin: in "Proceedings of the 7th International Congress on Marine Corrosion and Fouling", Valencia, Spain (1988).

[2] R. Holthe, E. Bardal, P. O. Gartland: in "Proceedings Corrosion/88", NACE, Houston, TX No. 393 (1988).

[3] R. Johnsen, E. Bardal: Corrosion 41 (1985) 296.

[4] H. A. Videla, M. F. L. de Mele, G. Brankevich: in "Proceedings Corrosion/89", NACE, Houston, TX, No. 291 (1989).

[5] F. Mansfeld, B. Little: in "Proceedings Corrosion/90", NACE, Houston, TX, No. 108 (1990).

[6] F. Mansfeld, B. Little: A Technical Review of Electrochemical Techniques Applied to Microbiologically Influenced Corrosion. Corros. Sci. (in press).

[7] B. Little, P. Wagner, R. Ray, R. Pope, R. Scheetz: Biofilms: An ESEM Evaluation of Artifacts Introduced During SEM Preparation. submitted.

[8] F. Mansfeld, M. Kendig, W. Lorenz: J. Electrochem. Soc. 132 (1985) 290.

[9] F. Mansfeld, C. H. Tsai, H. Shih, B. Little, R. Ray, P. Wagner: in "Proceedings Corrosion/90". NACE. Houston.TX, No. 109 (1990).

[10] F. Mansfeld, C. H. Tsai, H. Shih, B. Little, R. Ray, P. Wagner: An Electrochemical and Surface Analytical Study of Stainless Steels and Titanium Exposed to Natural Seawater, submitted.

[11] H. Shih, F. Mansfeld: "Software for Quantitative Analysis of Polarization Curves", Proc. Symp. on "Computer Modeling for Corrosion", ASTM. San Antonio, TX, Nov. 1990 (in press).

[12] S. M. Gerchakov, L. R. Udey, F. Mansfeld: Corrosion 37 (1981) 696.

[13] B. Little, R. Ray, P. Wagner, F. Mansfeld, R. Tsai, H. Shih: in Proc. Symp. "Application of Surface Analysis Methods to Environmental Material Interactions". The Electrochem. Soc. Seattle, WS. Oct. 1990 (in press).

[14] P. Duncumb, S. J. B. Reed: "Quantitative Electron Probe Microanalysis", K. F. J. Heinrich, Editor, p. 133, NBS Special Publication 298 (1968).

[15] K. F. J. Heinrich: in "Proc. 11th International Conference, X-Ray Optics and Microanalysis", London, Ont. (1986).

[16] B. L. Henke, P. Lee, T. J. Tanaka, R. L. Shimabukuro, B. K. Fujikawa: Atomic Data and Nuclear Data Tables 27 (1982) 1.

[17] D. R. Beaman, J. A. Isasi: "Electron Beam Microanalysis", ASTM STP 506, Philadelphia, PA. (1974).

[18] C. Kato, B. G. Ateya, J. E. Castle, H. W. Pickering: J. Electrochem. Soc. 127 (1980) 1890.

[19] R. J. K. Wood, S. P. Hutton, D. J. Schiffrin, Corr. Sci. 30 (1990) 1177.

[20] A. Mollica, A. Trevis: in "Proceedings 4th International Congress on Marine Corrosion and Fouling", Antibes, France (1976).

[21] V. Scotto, R. DiCintro, G. Marcenaro: Corrosion Sci. 25 (1985) 185.

[22] S. C. Dexter, G. Y. Gao: Corrosion 44 (1988) 717.

[23] P. J. B. Scott, J. Goldie, M. Davies: Mat. Perf. 30 (1) (1990) 55.

[24] A. Mollica, A. Trevis, E. Traverso, G. Ventura, G. DeCarolis, R. Dellepiane. Corrosion 45 (1980) 48.

[25] A. Mollica, G. Ventura, E. Traverso, V. Scotto. Int. Biodeterior. 24 (1988) 221.

[26] B. Little, R. Ray, P. Wagner, Z. Lewandowski, W. C. Lee, W. G. Characklis, F. Mansfeld: Impact of Biofouling on the Electrochemical Behaviour of 304 Stainless Steel in Natural Seawater (in press).

[27] C. Kato, H. W. Pickering: J. Electrochem. Soc. 131 (1984) 1219.

[28] S. R. Sánchez, D. J. Schiffrin: Corr. Sci. 22 (1982) 585.

[29] F. Mansfeld, J. V. Kenkel: Corrosion 33 (1977) 376.

[30] W. C. Chen, Atrens: in "Step Into the 90's", Vol. 3, Queensland, Australasian Institute of Metal Finishing, Parkville, Victoria, Australia (1989).

[31] S. M. Gerchakov, F. J. Roth, B. Sallman, D. S. Marszalek: in "Proceedings of the Ocean Thermal Energy Conversion (OTEC) Biofouling and Corrosion Symposium", R. H. Gray, Editor, U.S. Department of Energy (1977).

[32] F. Mansfeld, M. Kendig, S. Tsai: Corrosion 38 (1982) 478.

[33] G. F. Daniel, A. H. L. Chamberlain: Botanica Marina 24 (1981) 229.

[34] D. S. Marszalek, S. M. Gerchakov, L. R. Udey: Appli. Environ. Microbiol. 38 (1979) 987.

[35] J. M. Popplewell: in "Proceedings Corrosion/78". NACE, Houston, TX, No. 21 (1978).

[36] D. C. Vreeland, E. G. Odgen: "Seawater Corrosion of 90/10 Copper-Nickel Piping – Survey". Naval Ship Research and Development Center, Annapolis, MD. Report TM28-74-307 (1974).

[37] D. H. Pope, D. J. Duquette, A. H. Johannes, P. C. Wayner. Mater. Performance 23 (1984) 14.

[38] B. C. Syrett, D. D. Macdonald, S. S. Wing: Corrosion 35 (1979) 409.

[39] G. G. Geesey, M. W. Mittleman, T. Iwaoka, P. R. Griffiths: Mater. Performance 25 (1986) 37.